Mössbauer absorption and emission study of dilute Fe^{2+} impurities in cubic ZnS. Observation of metastable electronic levels. I. Relaxation measurements

P. Bonville, C. Garcin, A. Gérard,* P. Imbert, and G. Jéhanno
Service de Physique du Solide et de Résonance Magnétique, Centre d'Etudes Nucléaires de Saclay, 91191 Gif-sur-Yvette Cèdex, France

(Received 28 May 1980)

In dilute ZnS:^{57}Fe absorbers the isolated Fe^{2+} ions give a single Mössbauer absorption line at all temperatures ($1.4 \leq T \leq 295$ K), but a relaxation broadening is observed near 8 K. A convenient relaxation line-shape theory has enabled the transition rate $W_{\Gamma_4 \to \Gamma_1}$ from the first excited spin-orbit triplet Γ_4 to the ground-state level Γ_1 to be measured between 6 and 13 K. Two additional Fe^{2+} quadrupole doublets appear for $T \lesssim 5$ K in the ZnS:^{57}Co emission spectra. These are due to the slow relaxation contributions of the excited spin-orbit triplets Γ_4 and Γ_5 of Fe^{2+} which are then observed out of the thermal equilibrium following the decay of the radioactive parent ^{57}Co. The two transition rates $W_{\Gamma_4 \to \Gamma_1}$ and $W_{\Gamma_5 \to \Gamma_1}$ were obtained by following the intensities of the Γ_4 and Γ_5 lines in the emission spectra below 5 K when these rates are comparable to the inverse nuclear lifetime $1/\tau$. Both the absorber and source measurements of $W_{\Gamma_4 \to \Gamma_1}$ show approximately a $T^{5.0}$ mean thermal variation, whereas the source measurements of $W_{\Gamma_5 \to \Gamma_1}$ present a $T^{4.0}$ mean variation. These relaxation rates are attributed to Raman processes, which have been shown to follow the thermal dependence $W_{e \to g} \propto (\hbar\omega_0)^7[6!(k_B T/\hbar\omega_0)^7 + (3)(5!)(k_B T/\hbar\omega_0)^6 + (3)(4!)(k_B T/\hbar\omega_0)^5 + 3!(k_B T/\hbar\omega_0)^4]$ instead of the usual T^7 dependence, when the temperature is smaller than the energy separation $E_e - E_g = \hbar\omega_0$ between the excited level and the ground-state level.

I. INTRODUCTION

In a review paper on spin relaxation in solids and aftereffects of nuclear transformations,[1] Wickman and Wertheim mentioned in 1968 the considerable interest which would result from observing quasi-metastable atomic or ionic levels populated by the preceding nuclear event by Mössbauer emission spectroscopy.

We present here the first unambiguous observation and the detailed study of electronic levels which are populated out of the thermal equilibrium after the radioactive decay in a Mössbauer source. Although these levels are low-lying excited levels which can be easily thermally populated in conventional absorption experiments, they are observable at the slow relaxation limit only in emission spectroscopy near zero kelvin when their populations lie out of equilibrium. We took advantage of this situation to study their hyperfine and vibronic properties, and to measure the transition rates from these levels towards the ground-state level in an unconventional way.

These properties were observed on iron impurities in the cubic phase of ZnS (blende). More precisely, the study concerns Fe^{2+} ions which are substituted for Zn^{2+} ions in regular tetrahedral sites, and which are sufficiently diluted to be considered as being isolated impurities in the matrix.

We have already pointed out that the low-temperature Mössbauer spectra of such Fe^{2+} ions were remarkably different when obtained from dilute ZnS:^{57}Fe absorbers and when obtained from ZnS:^{57}Co sources.[2] Namely, below about 5 K, the single line emitted by the Fe^{2+} ions in the ZnS:^{57}Co sources gives rise to three distinct contributions, i.e., one central line and two quadrupole doublets, whereas only one Fe^{2+} absorption line is observed in the absorber spectra at all temperatures ($1.4 \leq T \leq 295$ K).

(N.B. The source spectra also contain a small additional contribution which is visible below 255 K and which we attributed to the charge state Fe^{1+}. We will not further consider here this abnormal charge state, as its behavior has already been described elsewhere.[3])

Theoretical predictions concerning the low-temperature Mössbauer spectra of Fe^{2+} in ZnS were made by Ham in 1974.[4] Ham showed that the slow relaxation contribution of the first excited spin-orbit triplet Γ_4 of Fe^{2+}, when slightly separated by random strains, should be a quadrupole doublet with a

separation $\Delta E_Q(\Gamma_4) \simeq 3$ mm s^{-1}.

However this doublet cannot be observed in the absorber experiments, because the slow relaxation limit is attained only at temperatures where the population of the Γ_4 level is too small to be detected.

In the source experiments however, a finite metastable population is observed down to 0 K in the level Γ_4,[2] because a complete thermalization of this level after the decay of ^{57}Co would require a time longer than the nuclear lifetime τ which is characteristic of the Mössbauer emission. The slow relaxation contribution of the level Γ_4 is then visible in the emission spectra below 5 K, where it forms the largest (or external) quadrupole doublet.

Although we have established that the second (or internal) quadrupole doublet originates in a very similar way from the second excited spin-orbit triplet Γ_5, which is also populated out of the thermal equilibrium, this assignment was not immediately obvious and was proposed only later.[5] The difficulty was that both levels Γ_4 and Γ_5 were thought at first to give the same quadrupole splitting, as predicted by the crystal-field theory modified by a weak dynamical Jahn-Teller effect calculated within the usual approximations.[2,4] But a more refined treatment of the vibrational properties, which is described in the next paper (Part II), accounts for the observed differences between the two quadrupole doublets and leads to the evaluation of the dynamical Jahn-Teller effect in the ^5E state of Fe^{2+} in ZnS.

In the present paper labeled Part I, we give a comprehensive description of the absorber and source experiments on Fe^{2+} in ZnS, and of the relaxation processes amongst the electronic levels which govern the differences between absorption and emission spectra.

The sample preparation and the experimental conditions are described in Sec. II. In Sec. III the energy-level diagram of the Fe^{2+} ion in symmetric tetrahedral coordination is given together with the corresponding hyperfine interactions. Section IV deals with the results of the absorber experiments and the corresponding relaxation measurements. A theoretical relaxation line shape is calculated and used to deduce the transition rate $W_{\Gamma_4 \to \Gamma_1}$ (labeled W_4) from the broadened absorption spectra between 6 and 13 K. In Sec. V the emission spectra are described and the transition rates $W_{\Gamma_4 \to \Gamma_1}(W_4)$ and $W_{\Gamma_5 \to \Gamma_1}(W_5)$ are derived, respectively, from the Γ_4 and Γ_5 line intensities in the spectra below 5 K. The origin of these relaxation rates is discussed in terms of Raman processes. The theoretical thermal dependence of these processes is reexamined here for the particular case where the temperatures involved are lower than the energy separation between the relaxing levels. In the conclusion (Sec. VI), the relaxation data are shown to support the interpretation of the emission spectra in terms of metastable populations within the Γ_4 and Γ_5 levels. Some original aspects of the present study are emphasized and possible extensions are examined.

II. SAMPLE PREPARATION AND EXPERIMENTAL ARRANGEMENT

A. Absorber sample ($Zn_{0.998}{}^{57}Fe_{0.002}$ S)

First pure ZnS blende powder was prepared by heating the constituents with some excess of sulphur in a vacuum sealed silica tube at 900 °C for about 100 h. The $Zn_{0.998}{}^{57}Fe_{0.002}$ S sample was prepared in two steps, by initially reheating in the same way 2 mol% of the mixture (^{57}Fe + S) with 98 mol% of ZnS, and then by further solid dilution at 900 °C into ZnS. In order to prevent oxidation into Fe^{3+} it was necessary to keep the sample in the presence of a dehydrating agent and to avoid the use of oxidizing glue when sealing the sample inside the sample holder. In spite of these precautions a few percent of Fe^{3+} ions were detected (Sec. IV). Such an oxidation was not observed when the initial experiments were carried out.[2]

B. Source sample (ZnS:^{57}Co)

Different preparation modes have been tested[3] and all of them were found to give samples with essentially the same low-temperature Fe^{2+} emission spectra.

The sample used in the present study was prepared from a ZnS powder synthesized at 700 °C. The powder was wetted with a solution of $^{57}CoCl_2$ in 0.1 N HCl, and a $S(NH_4)_2$ solution was added for precipitating ^{57}Co as a sulphide. After desiccation and vacuum evaporation of $Cl(NH_4)_2$ at 200 °C, the diffusion of ^{57}Co in ZnS was performed at 700 °C for 15 h. The activity of the source was 3 to 4 mCi.

C. Experimental arrangement

The absorption spectra of the ^{57}Fe doped ZnS sample were recorded using a moving reference source of ^{57}Co in rhodium, and the emission spectra of the ^{57}Co doped ZnS sample were recorded using a moving reference absorber made of potassium ferrocyanide containing 0.1 mg of ^{57}Fe per cm^2. The linewidth of this absorber, as calibrated with the ^{57}Co-Rh source, was about 0.24 mm s^{-1}.

A symmetrical sawtooth velocity signal was used and the base line distortion was corrected by folding the double spectrum. Special care was taken in order to avoid parasitic vibrations in the experimental setup when observing the relaxation linewidth anomaly in the low-temperature experiments.

III. ELECTRONIC LEVELS AND HYPERFINE INTERACTIONS

The energy-level diagram of the Fe^{2+} ion in tetrahedral cubic symmetry sites (point group T_d) is given in Fig. 1. The lowest term ^5D of the Fe^{2+} ($3d^6$) free ion is split by the cubic crystal field into a ground-state orbital doublet ^5E and an excited orbital triplet $^5T_2$ separated by $\Delta = 3400$ cm^{-1} for Fe^{2+} in ZnS.[6] The doublet is split in turn by the spin-orbit and the spin-spin interactions, and to within the accuracy of second-order perturbation theory it gives rise to five uniformly spaced levels ($\Gamma_1, \Gamma_4, \Gamma_3, \Gamma_5, \Gamma_2$) separated by the energy interval[7]

$$\delta_{so} = 6[(\lambda^2/\Delta) + \rho] \quad . \tag{3.1}$$

λ is the spin-orbit coefficient (free ion value $\lambda_0 = -100 \pm 10$ cm^{-1}); ρ, the effective spin-spin parameter, is equal to $+0.95$ cm^{-1} according to Pryce.[8] The value of δ_{so} corresponding to $\lambda = \lambda_0$ and $\Delta = 3400$ cm^{-1} would be 23.3 cm^{-1}.

As shown by Ham[4] a moderate Jahn-Teller coupling in the ^5E state with a vibrational mode $\hbar\omega >> 4\delta_{so}$ reduces the energy interval, which then becomes

$$\delta = \delta_{so} q = 6q[(\lambda^2/\Delta) + \rho], \quad q < 1 \quad . \tag{3.2}$$

However, experimentally it is difficult to distinguish this energy reduction due to the dynamical Jahn-Teller effect from the effect resulting from reductions in λ and ρ as a consequence of covalency. δ is found experimentally to be 15.0 ± 0.1 cm^{-1} for Fe^{2+} in ZnS.[9]

The two singlets Γ_1 and Γ_2 as well as the doublet Γ_3 are diamagnetic levels and do not give rise to either a magnetic or a quadrupolar hyperfine interaction in a cubic tetrahedral site.

For the triplet Γ_4, Ham has pointed out both the effect of random strains and the role of the dynamical Jahn-Teller coupling.[4] The local strains, which always exist in the actual samples, split this triplet into three diamagnetic singlets Γ_{4x}, Γ_{4y}, and Γ_{4z}, each of them giving rise to the same quadrupole splitting energy. The value of this common energy, which is reduced by the Jahn-Teller factor q, is given by

$$\Delta E_Q = 6q|C_E|, \quad C_E = \tfrac{1}{7}\langle r^{-3}\rangle e^2 Q/[I(2I-1)] \quad . \tag{3.3}$$

This expression holds for strain separations much smaller than δ, and ΔE_Q is then a strain independent quadrupole interaction, which should be observable at the slow relaxation limit.

For large electronic transition rates compared to the quadrupole energy ΔE_Q, the quadrupole interaction should vanish by relaxation averaging because of the compensation between the electric field gradients (EFG) corresponding to the three sublevels Γ_{4x}, Γ_{4y}, and Γ_{4z}.

All these predictions concerning the triplet Γ_4 can be extended to the triplet Γ_5. The present experimental study however showed that the reduction factor q in relation (3.3) is not the same for the levels Γ_4 and Γ_5, which rules out the possibility of describing the dynamical Jahn-Teller effect by means of a unique reduction factor q within all the spin-orbit sublevels of the ^5E orbital doublet.

In order to observe the quadrupole doublet due to the first excited triplet Γ_4, Ham suggested studying ZnS:^{57}Fe absorbers around 10 K, i.e., at temperatures high enough to appreciably populate the level Γ_4, but low enough to possibly avoid fast relaxation effects.

In fact the slow relaxation quadrupole doublet has not been observed in absorber experiments as the relaxation rate remains too high even when the temperature is lowered such that the Γ_4 level is only very slightly populated (Sec. IV). On the contrary the slow relaxation doublets due to the excited triplets Γ_4 and Γ_5 are apparent near 0 K in the emission spectra because of the existence of metastable populations in these levels after the radioactive decay of ^{57}Co (Sec V).

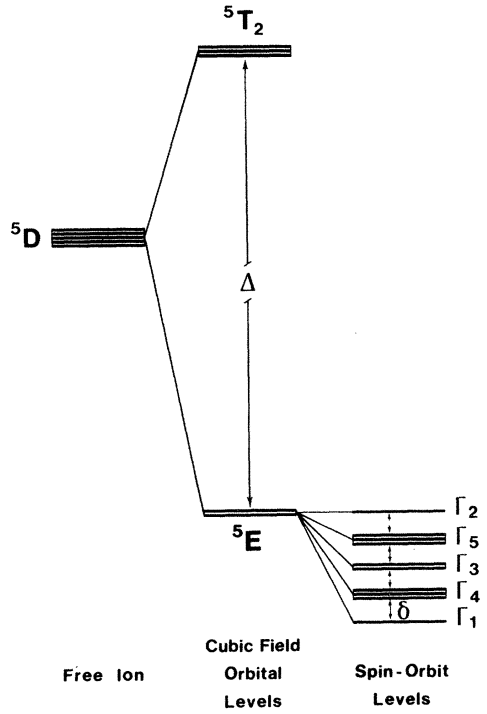

FIG. 1. Electronic level diagram of the Fe^{2+} ion in a regular tetrahedral site. ($\Delta \simeq 3400$ cm^{-1} and $\delta \simeq 15$ cm^{-1} for Fe^{2+} in ZnS.)

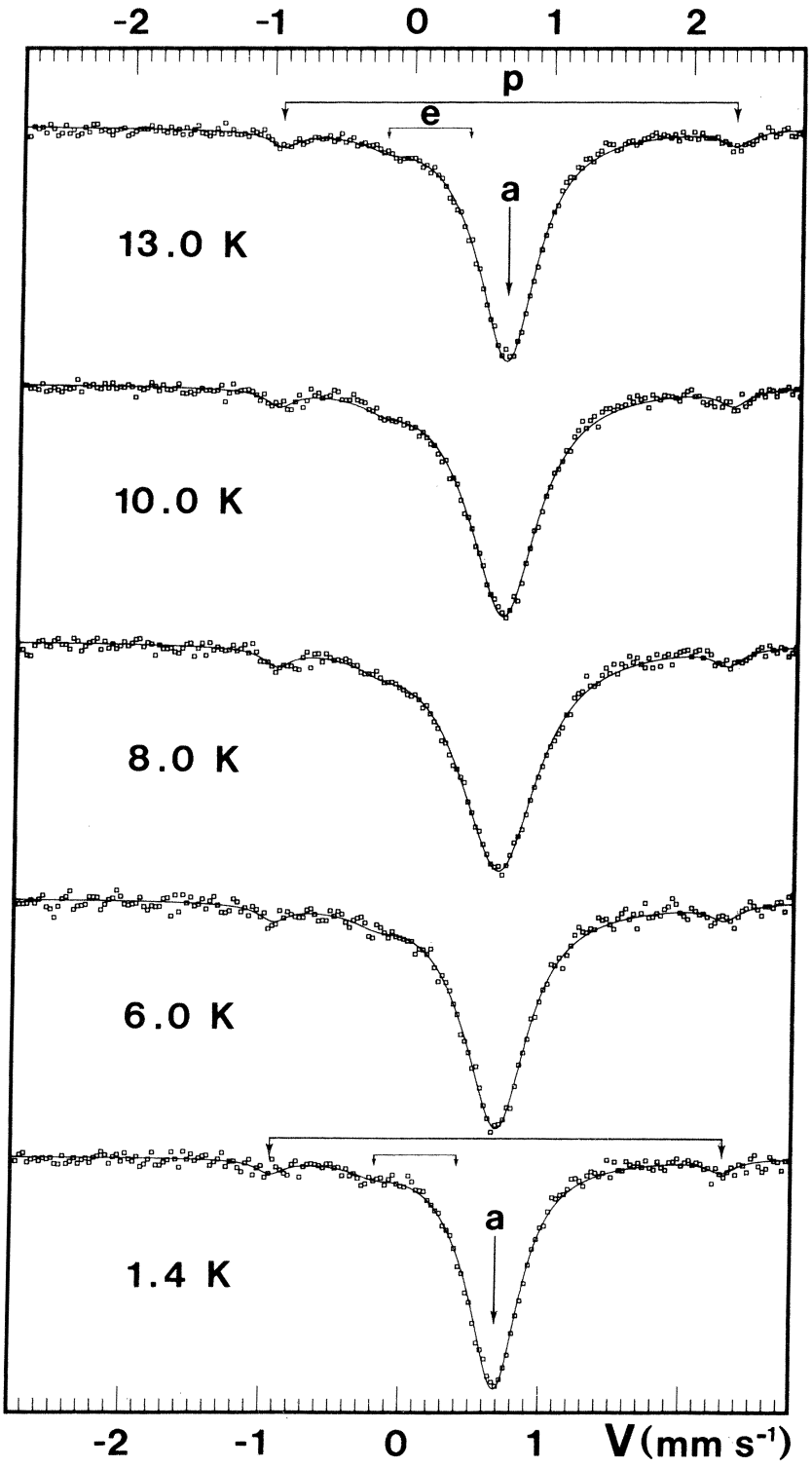

FIG. 2. Fe^{2+} Mössbauer absorption spectra of $Zn_{0.998}{}^{57}Fe_{0.002}S$ and fitted curves. *a*: main line (~88.5%) due to isolated Fe^{2+} impurities, fitted using a relaxation line shape (Sec. IV). *p*: quadrupole doublet (~5.5%) due to Fe^{2+}-Fe^{2+} pairs. *e*: quadrupole doublet (~6%) due to Fe^{3+} ions (partial oxidation of the sample).

IV. ABSORBER EXPERIMENTS AND RELAXATION MEASUREMENTS

Preliminary results have already been described[2]: Isolated Fe^{2+} impurities gave a single Mössbauer absorption line at all temperatures ($1.35 \leq T \leq 295$ K) but the linewidth went through a sharp maximum at near 8 K. This line broadening was attributed to relaxation effects involving the first excited spin-orbit level, the triplet Γ_4. A brief initial analysis of the relaxation line shape has also been given.[10]

A. Experimental results

New and detailed Mössbauer experiments have been carried out on the $Zn_{0.998}{}^{57}Fe_{0.002}$ S sample between 1.4 and 13 K. Some spectra and fitted curves are given in Fig. 2. In addition to the main line (a) due to isolated Fe^{2+} impurities, all the spectra show two small additional contributions.

(i) *A quadrupole doublet (p) due to Fe^{2+} ion pairs,* with the following characteristics at 4.2 K: isomer shift $S = 0.67 \pm 0.02$ mm s^{-1} referred to the ^{57}Co-Rh source; quadrupole splitting $\Delta E = 3.23 \pm 0.04$ mm s^{-1}. As the relative intensity of this doublet is constant from 1.4 to 13 K ($5.5 \pm 2\%$) it cannot represent the slow relaxation contribution of the excited level Γ_4 whose population is completely negligible at 1.4 K. And in fact its characteristics and their thermal variation unambiguously show that this quadrupole doublet is due to Fe^{2+} ions associated in pairs of next-nearest neighbors.[11]

(ii) *A quadrupole doublet (e) due to Fe^{3+} ions.* This doublet has the following characteristics at 4.2 K: $S = 0.09 \pm 0.02$ mm s^{-1} (refer to ^{57}CoRh); $\Delta E = 0.59 \pm 0.04$ mm s^{-1}; the relative intensity is $6 \pm 2\%$ at all temperatures. We attribute this doublet to a slight oxidation of the sample.

As concerns the isolated Fe^{2+} ions, the observations are as follows.

(i) *These ions contribute a single absorption line (a) at all temperatures.* The isomer shift of this line is $S = 0.537 \pm 0.01$ mm s^{-1} at 295 K and $S = 0.67 \pm 0.01$ mm s^{-1} at 4.2 K (refer to ^{57}Co-Rh).

The Γ_4 excited triplet does not contribute a slow relaxation quadrupole doublet, which contrasts with the case of the system CaF_2:$^{57}Fe^{2+}$.[12,13] This is due to the fact that the slow relaxation between the electronic levels in ZnS:$^{57}Fe^{2+}$ is achieved only at temperatures where the Γ_4 level is much too depopulated to give a visible absorption in the Mössbauer spectrum.

(ii) The linewidth of the single line, which has been fitted using a Lorentzian line shape, shows a steady increase from room temperature to about 5 K, and a superposed peak at 8 K (Fig. 3). The steady increase is due to small strain-induced electric field gradients within the spin-orbit levels and particularly the ground-state singlet Γ_1.[4,11]

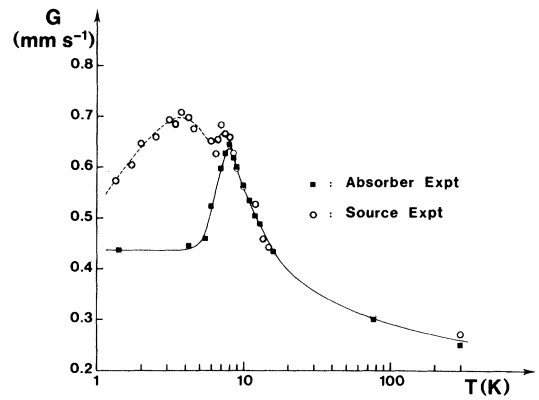

FIG. 3. Fe^{2+} Mössbauer linewidth vs temperature. Black squares: from absorption spectra; and open circles: from emission spectra (central linewidth). Source and absorber results are identical above 8 K where the thermal equilibrium within the Fe^{2+} electronic levels holds in both samples, but not at lower temperatures where the Γ_4 and Γ_5 populations depart from the equilibrium in the source.

The additional peak in the line broadening which occurs between 5 and 15 K and which reaches a maximum value at 8 K results from the contribution of the excited triplet Γ_4 in the intermediate relaxation range. This relaxation broadening disappears below 5 K because of the depopulation of Γ_4, and above 15 K because of fast relaxation averaging. We develop below the relaxation line-shape theory which provides a quantitative interpretation of this linewidth anomaly.

B. Relaxation line-shape theory

In 1967, in order to interpret the relaxation spectra of Fe^{2+} in MgO in octahedral coordination,[14–17] Tjon and Blume developed a stochastic theory of the Mössbauer line shape.[18] For that purpose they used a fluctuating quadrupole Hamiltonian which contains an axial EFG fixed in magnitude, but randomly jumping between the x, y, and z axes.

In order to extend this model to our problem, we must take into account the differences between the octahedral and the tetrahedral symmetries. In the octahedral site the three equivalent EFG's originate from the sublevels of the spin-orbit triplet Γ_{5g} which is the ground state level. However, in the tetrahedral site they originate from an excited level, the triplet Γ_4. As long as the strain separation is small compared to the spin-orbit separation, the sublevels Γ_{4x}, Γ_{4y}, and Γ_{4z} are the eigenstates whatever the nature

of the strain, and they induce equivalent axial EFG's, respectively, along the Ox, Oy, and Oz axes. The ground-state level in the present case is a singlet Γ_1 for which the very small quadrupole interaction, due to the strain mixing of the states Γ_1 and Γ_3, can be neglected in a first approximation. We must therefore include the value zero amongst the possible values of the fluctuating EFG. We must also take into account the respective populations of the levels Γ_1 and Γ_4 at the Boltzmann equilibrium, as well as the possible transition rates between these levels and within the triplet Γ_4. We will neglect the upper levels Γ_3, Γ_5, and Γ_2 which are not significantly populated in the considered temperature range ($T \leq 13$ K). The fluctuating quadrupole Hamiltonian may then be written as

$$\mathcal{H}(t) = q|C_E|[1-(\tfrac{1}{4})f^2(t)]\{[1-f^2(t)][3I_z^2-I(I+1)]+\tfrac{2}{3}f(t)[1+f(t)][3I_x^2-I(I+1)] - \tfrac{2}{3}f(t)[1-f(t)][3I_y^2-I(I+1)]\} , \tag{4.1}$$

where the random function of time $f(t)$ takes on the four possible values 2, 1, 0, and -1 corresponding, respectively, to an EFG which is zero, or which has three equivalent finite values along the x, z, and y axes. These finite values correspond to the quadrupole interaction given in relation (3.3).

$\mathcal{H}(t)$ may be rewritten as

$$\mathcal{H}(t) = V_1 f_1(t) + V_2 f_2(t) \tag{4.2}$$

with

$$\begin{cases} V_1 = \frac{1}{2}q|C_E|[3I_z^2 - I(I+1)] \\ V_2 = \frac{3}{4}q|C_E|(I_+^2 + I_-^2) \end{cases} ,$$

$$\begin{cases} f_1(t) = 2[1 - \frac{23}{12}f^2(t) + \frac{5}{12}f^4(t)] \\ f_2(t) = \frac{1}{3}[4f(t) - f^3(t)] \end{cases} .$$

Using the usual convention,[19] we define the relaxation matrix $\mathcal{W}$ by the stochastic matrix whose off-diagonal elements $\langle a|\mathcal{W}|b\rangle$ are equal to the probability per unit time that $f(t)$ makes a transition from a to b, and whose diagonal elements are $\langle a|\mathcal{W}|a\rangle = -\sum_{b\neq a}\langle a|\mathcal{W}|b\rangle$. In comparison with the matrix used by Tjon and Blume[18] the present relaxation matrix is more complex as it involves two distinct relaxation mechanisms. Namely, in addition to the transition rate W_4' from any sublevel to another sublevel inside the triplet Γ_4, we include a second transition rate W_4 from any Γ_4 sublevel to the ground-state level Γ_1. In addition the opposite transition rate from Γ_1 to each of the Γ_4 sublevels involves the Boltzmann factor of the level Γ_4 and is equal to $W_4E = W_4\exp(-\delta/k_BT)$. The relaxation matrix $\mathcal{W}$ is then written as follows:

$f(t)$	2	1	0	−1
2	$-3W_4E$	W_4E	W_4E	W_4E
1	W_4	$-W_4-2W_4'$	W_4'	W_4'
0	W_4	W_4'	$-W_4-2W_4'$	W_4'
−1	W_4	W_4'	W_4'	$-W_4-2W_4'$

(4.3a)

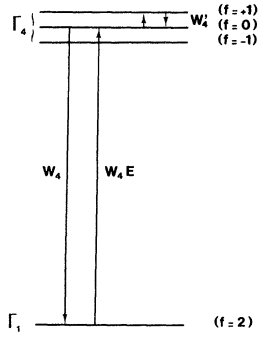

(4.3b)

A straightforward generalization of relation (15) of Ref. 18 gives the line shape

$$I(\omega) \propto \mathrm{Re}\sum_{i,j,m_1}\langle j|\mathfrak{A}(p)[1+3\alpha^2(m_1)\mathfrak{B}(p)\mathfrak{A}(p)]^{-1}P|i\rangle , \tag{4.4}$$

with $p = -i\omega + \frac{1}{2}\Gamma$,

$$\alpha(m_1 = \pm\tfrac{1}{2}) = \tfrac{3}{2}q|C_E|, \quad \alpha(m_1 = \pm\tfrac{3}{2}) = -\tfrac{3}{2}q|C_E| ,$$

$$\mathfrak{A}(p) = [p - i\alpha(m_1)\mathfrak{F}_1 - \tilde{\mathcal{W}}]^{-1},$$

$$\mathfrak{B}(p) = \mathfrak{F}_2[p + i\alpha(m_1)\mathfrak{F}_1 - \tilde{\mathcal{W}}]^{-1}\mathfrak{F}_2 .$$

$\mathfrak{F}_1$ and $\mathfrak{F}_2$ are diagonal matrices whose elements

are, respectively, the allowed values of $f_1(t)$ and $f_2(t)$:

$$\mathfrak{F}_1=\begin{pmatrix}0 & & & \\ & -1 & & \\ & & 2 & \\ & & & -1\end{pmatrix},\quad \mathfrak{F}_2=\begin{pmatrix}0 & & & \\ & 1 & & \\ & & 0 & \\ & & & -1\end{pmatrix}$$

and P is the density matrix of the electronic system

$$P=\frac{1}{1+3E}\begin{pmatrix}1 & & & \\ & E & & \\ & & E & \\ & & & E\end{pmatrix},\quad \text{with } E=\exp(-\delta/k_BT)\ .$$

Finally $\tilde{\mathfrak{W}}$ represents the transposed matrix of the relaxation matrix $\mathfrak{W}$ [N.B. We note that it is $\tilde{\mathfrak{W}}$ and not $\mathfrak{W}$ that should have been used in the expression of $\mathfrak{A}(p)$ and $\mathfrak{B}(p)$ given in Ref. 18. This slight error however did not affect the final result (16) of Tjon and Blume because only a symmetrical $\mathfrak{W}$ matrix was then used.]

In order to compute the line shape expression (4.4) three 4×4 matrices have to be inverted.

We also used another method for calculating the relaxation line shape, starting from the formalism given by Blume and based on Liouville operators.[19]

This latter formalism requires the calculation of the supermatrix elements $\langle I_0m_0I_1m_1a|(p\,1-\mathfrak{W}-i\sum_j V_j^xF_j)^{-1}|I_0m_0'I_1m_1'b\rangle$ [Blume, relation (22)]. As the quadrupole Hamiltonian $\mathfrak{IC}(t)$ does not act within the nuclear ground state of ^{57}Fe, we must have $m_0=m_0'$, and from the reciprocal nature of the associated transition operator matrix elements $\langle I_1m_1|\mathfrak{IC}^{(-)}|I_0m_0\rangle$ and $\langle I_0m_0|\mathfrak{IC}^{(+)}|I_1m_1'\rangle$, it follows also that $m_1=m_1'$. After summing over m_0 and over the different transition operators $\mathfrak{IC}_{LM}(M=1,0,-1)$, Blume's relation (22) reduces to

$$I(\omega)\propto \mathrm{Re}\sum_{m_1ab}\left\langle I_1m_1a\left|p_a\left[p\,1-\mathfrak{W}-i\sum_j V_j^xF_j\right]^{-1}\right|I_1m_1b\right\rangle\ , \tag{4.5}$$

where p_a is the Boltzmann population of the electronic state corresponding to $f(t)=a$, and where the initial 32×32 matrix to be inverted reduces to the 8×8 matrix given in Table I. This reduction comes from the absence of the states $|I_0m_0\rangle$, and from a factorization into two identical matrices containing respectively, the states $m_1=\frac{3}{2},-\frac{1}{2}$ and $m_1=-\frac{3}{2},\frac{1}{2}$.

An elegant method for avoiding the matrix inversion at each frequency value ω has been given by Clauser[20]; it consists of using the closure relation $1/(p-\mathfrak{P})=\sum_\alpha[1/(p-p_\alpha)]|B_\alpha\rangle\langle C_\alpha|$ where p_α and $|B_\alpha\rangle$ are, respectively, the complex eigenvalues and eigenfunctions of the non-Hermitian operator $\mathfrak{P}=\mathfrak{W}+i\sum_j V_j^xF_j$, and $|C_\alpha\rangle$ the eigenfunctions of the conjugate operator $\mathfrak{P}^+$, with the normalization condition $\langle B_\alpha|C_\beta\rangle=\delta_{\alpha\beta}$. Using the properties of Liouville's operators, the line shape is then given by

$$I(\omega)\propto \mathrm{Re}\sum_{\alpha=1}^{8}\frac{1}{p-p_\alpha}\left[\left(\sum_a p_aB_\alpha(\tfrac{1}{2},\tfrac{3}{2},a)\right)\left(\sum_b C_\alpha^+(\tfrac{1}{2},\tfrac{3}{2},b)\right)+\left(\sum_a p_aB_\alpha(\tfrac{1}{2},-\tfrac{1}{2},a)\right)\left(\sum_b C_\alpha^+(\tfrac{1}{2},-\tfrac{1}{2},b)\right)\right]\ , \tag{4.6}$$

where $B_\alpha(\frac{1}{2},\frac{3}{2},a)$ is the component of $|B_\alpha\rangle$ along the state $(m_0=\frac{1}{2},m_1=\frac{3}{2},a)$, . . . ,.

The matrices $\mathfrak{P}$ and $\mathfrak{P}^+$ to be diagonalized are easily obtained from the 8×8 matrix $p\,1-\mathfrak{P}$ given in Table I.

We used this latter method for computing the line shape within Blume's formalism, and we checked that the line shapes given by Eqs. (4.4) and (4.6) were equivalent.

This relaxation line shape was first used successfully for fitting the relaxation spectra of the system CaF_2:$^{57}Fe^{2+}$,[21] where the eightfold-coordinated Fe^{2+} ion in cubic symmetry presents the same level scheme as Fe^{2+} in ZnS.

Fitting a given relaxation spectrum requires only two adjustable parameters, namely, the transition rates W_4 and W_4'. Theoretically both can be separately fitted, as they affect the line shape in a different way. The relaxation processes acting within the Γ_4 multiplet and corresponding to the rate W_4' modify the shape of the quadrupole doublet due to Γ_4, but do not broaden by themselves the single line due to Γ_1. In contrast the processes acting between Γ_4 and Γ_1 and involving the relaxation rate W_4 broaden both the quadrupole doublet due to Γ_4 and the central line due to Γ_1, before averaging them into a single line at higher temperatures. The possibility of fitting both W_4 and W_4' was clearly demonstrated

TABLE I. Matrix elements of the operator $p\,1-\mathcal{P}=p\,1-\mathcal{W}-i\sum_j V_j^x F_j$ which is used in the relaxation line-shape calculation (Sec. IV B). v is equal to $i\frac{3}{2}q|C_E|$, and $E=\exp(-\delta/k_BT)$.

	m_1	$a=2$		1		0		−1	
	m_1'	$\frac{3}{2}$	$-\frac{1}{2}$	$\frac{3}{2}$	$-\frac{1}{2}$	$\frac{3}{2}$	$-\frac{1}{2}$	$\frac{3}{2}$	$-\frac{1}{2}$
$b=2$	$\frac{3}{2}$	$p+3EW_4$		$-EW_4$		$-EW_4$		$-EW_4$	
	$-\frac{1}{2}$		$p+3EW_4$		$-EW_4$		$-EW_4$		$-EW_4$
1	$\frac{3}{2}$	$-W_4$		$p+W_4+2W_4'-v$	$v\sqrt{3}$	$-W_4'$		$-W_4'$	
	$-\frac{1}{2}$		$-W_4$	$v\sqrt{3}$	$p+W_4+2W_4'+v$		$-W_4'$		$-W_4'$
0	$\frac{3}{2}$	$-W_4$		$-W_4'$		$p+W_4+2W_4'+2v$		$-W_4'$	
	$-\frac{1}{2}$		$-W_4$		$-W_4'$		$p+W_4+2W_4'-2v$		$-W_4'$
−1	$\frac{3}{2}$	$-W_4$		$-W_4'$		$-W_4'$		$p+W_4+2W_4'-v$	$-v\sqrt{3}$
	$-\frac{1}{2}$		$-W_4$		$-W_4'$		$-W_4'$	$-v\sqrt{3}$	$p+W_4+2W_4'+v$

in the case of CaF_2:$^{57}Fe^{2+}$, where the experimental information is particularly rich, as the line shape varies from the slow relaxation limit to the fast relaxation limit. The situation however is less favorable in ZnS:$^{57}Fe^{2+}$, where only a relaxation broadening of the absorption line is observed.

C. Fitting results

The values of the constrained parameters were fixed as follows when fitting the relaxation spectra of ZnS:$^{57}Fe^{2+}$.

The separation δ between the levels Γ_1 and Γ_4, which is needed in the calculation of the Boltzmann factor $E=e^{-\delta/k_BT}$, was fixed at 15 cm^{-1}.[9]

The limiting linewidth in the absence of relaxation was fixed at $G_0=0.436$ mm s^{-1}, which is the experimental linewidth at 1.4 K. In this way the static broadening of the line due to small strain-induced quadrupole effects in the Γ_1 ground-state level was taken into account.

For the quadrupole splitting in the triplet Γ_4, we used $\Delta E_Q(\Gamma_4)=q(\Gamma_4)6|C_E|=3.0$ mm s^{-1} as observed in the source experiments (Sec. V).

The spectrum at 8 K, which presents the largest relaxation broadening, was first analyzed in various different ways.

Unphysical negative values of W_4' were obtained first when both W_4 and W_4' were considered as adjustable parameters. Further attempts showed that the spectrum was easily fitted by W_4 only, with W_4' fixed at zero [Fig. 4(a)], while the alternative solution ($W_4=0$; W_4' adjustable) gave a very poor fit [Fig. 4(b)]. Additional fits with W_4 free and W_4' fixed at different finite values revealed that W_4 *was at least ten times larger than* W_4'. Under these conditions we assumed that W_4' was negligibly small compared to W_4, and we fitted the whole range of relaxation spectra by adjusting W_4 with W_4' fixed at zero. As a conclusion we can say that the line broadening in ZnS:$^{57}Fe^{2+}$ is due to the transitions between the level Γ_4 and the level Γ_1, while in CaF_2:$^{57}Fe^{2+}$ the dominant relaxation mechanism is due to the transitions between the Γ_4 sublevels themselves ($W_4' > W_4$).[21]

During this fitting procedure we encountered the following difficulty: Depending on the initial values attributed to W_4 the program converged towards two distinct values $W_4(1)$ and $W_4(2)$ [$W_4(1) < W_4(2)$],

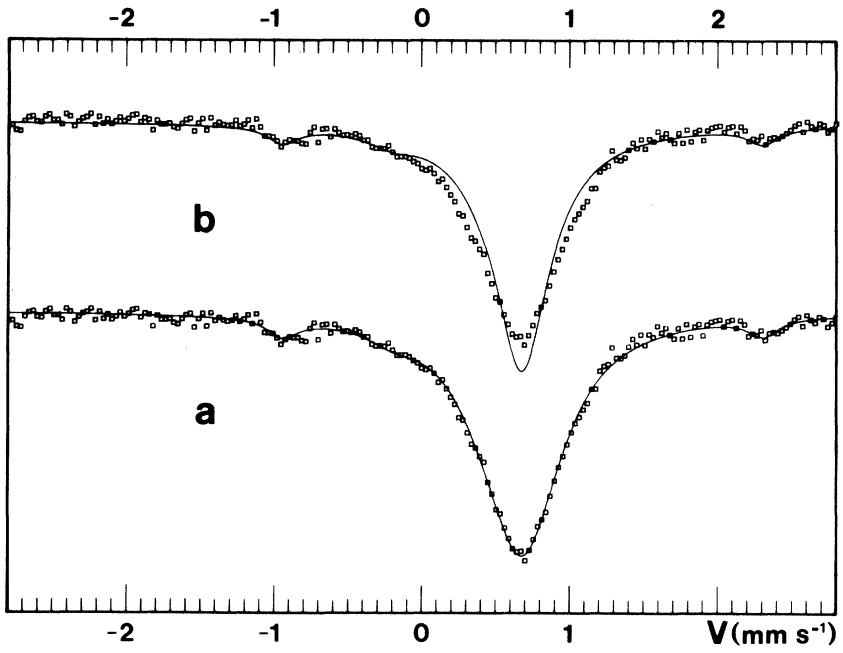

FIG. 4. Absorption spectrum of $ZnS:_{0.998}{}^{57}Fe_{0.002}S$ at 8 K fitted with two different hypotheses. *a*: W_4 adjustable, $W_4' = 0$; and *b*: W_4' adjustable, $W_4 = 0$.

each of them giving approximately the same mean-square difference between experimental and theoretical line shapes below 8 K. However the ambiguity was removed by requiring that W_4 must increase with temperature. The correct values correspond then to $W_4(1)$ for $T \leq 6$ K, and to $W_4(2)$ for $T \geq 7.5$ K. The $W_4(2)$ values give also a much better fit to the experimental line shape above 8 K. But between 6 and 7.5 K where the change occurs between $W_4(1)$ and $W_4(2)$, no precise determination of W_4 is possible.

As W_4 measurements become hazardous below 6 K and above 13 K where the relaxation broadening vanishes, the fitted values of W_4 which may be considered as being significative correspond to the temperature range $7.5 \leq T \leq 13$ K and to the isolated value which has been measured at 6 K (Table II).

The variation of W_4 vs T between 6 and 13 K is given on a log-log plot in Fig. 5. The results approximately follow a straight line and the variation thus corresponds to a T^x-type law with $x \simeq 5.0$. (In a previous paper[10] we gave preliminary measurements of W_4 made only at four temperatures. These results initially seemed to be roughly compatible with a T^7-type law. However one of the measurements was made at 7 K and actually fell in the forbidden region between 6 and 7.5 K.)

TABLE II. Transition rate measurements.

T (K)	W_4 (10^6 s^{-1})	W_5 (10^6 s^{-1})	Observations
13.0	2250	· · ·	Absorber expt.
12.0	1597	· · ·	Absorber expt.
11.0	984	· · ·	Absorber expt.
10.0	657	· · ·	Absorber expt.
9.0	415	· · ·	Absorber expt.
8.5	326	· · ·	Absorber expt.
8.0	232	· · ·	Absorber expt.
7.5	213	· · ·	Absorber expt.
6.0	44.4	· · ·	Absorber expt.
4.6	16.7	83.7	Source expt.
4.2	7.53	55.5	Source expt.
3.8	4.99	37.7	Source expt.
3.4	2.95	25.4	Source expt.
3.2	2.61	17.8	Source expt.
3.1	2.59	15.7	Source expt.
3.0	1.33	12.6	Source expt.
2.5	· · ·	8.21	Source expt.
2.0	· · ·	3.62	Source expt.
1.7	· · ·	1.72	Source expt.

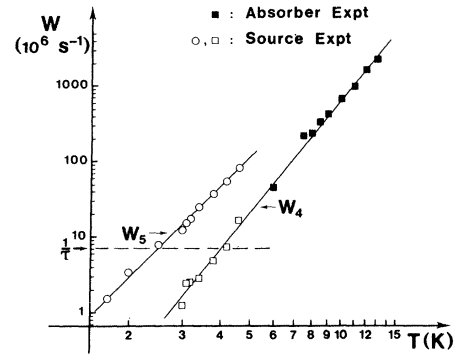

FIG. 5. Transition rates vs temperature. W_4: transition rate from the level Γ_4 towards the level Γ_1. [Black squares: absorber measurements; open squares: source measurements; straight-line curve: $W_4(s^{-1}) = 6.77 \times 10^3 T^{5.0}$ fitted variation.] W_5: transition rate from the level Γ_5 towards the level Γ_1. [Open circles: source measurements; straight-line curve: $W_5(s^{-1}) = 0.178 \times 10^6 T^{4.0}$ fitted variation.] $1/\tau$ is the inverse nuclear lifetime of ^{57}Fe (14.4 keV).

The physical mechanism responsible for the relaxation rate W_4 will be discussed after the other W_4 values obtained from the source measurements have been given (Sec. V D).

The relaxation measurements in the ZnS:^{57}Fe absorber just mentioned lead to a very interesting consequence concerning the interpretation of the ZnS:^{57}Co emission spectra. The extrapolation towards lower temperatures of the straight line which has been observed between 6 and 13 K in the absorber (Fig. 5) shows that W_4 becomes smaller than the inverse nuclear lifetime $1/\tau = 7.09 \times 10^6$ s^{-1} of ^{57}Fe (14.4 keV) below about 4 K. As W_4 represents the depopulation rate of the level Γ_4 towards the ground-state singlet Γ_1, the result $W_4 \lesssim 1/\tau$ means that the population in the Γ_4 level—which is out of the thermal equilibrium in a source experiment just after the decay of the radioactive parent ^{57}Co—cannot reach its equilibrium value within the mean time τ required for the Mössbauer emission. The Γ_4 level should then behave as a metastable level below 4 K, and it should contribute a finite intensity to the emission spectra down to zero kelvin. As $W_4 < 1/\tau$ necessarily implies $W_4 << \Delta E_Q(\Gamma_4)$, the slow-relaxation condition is also fulfilled in the same temperature range. Consequently the slow relaxation quadrupole doublet of Γ_4, which is not visible in the absorption spectra, should then appear in the emission spectra at near 4 K when the temperature is lowered. As shown in the next section this is indeed what happens, and moreover the second excited triplet Γ_5 also contributes a quadrupole doublet to the low-temperature source spectra for similar reasons.

V. SOURCE EXPERIMENTS AND RELAXATION MEASUREMENTS

Using a ZnS:^{57}Co source of higher activity than in our previous experiments,[2] we recorded a number of spectra in two consecutive temperature ranges: (i) between 15 and 6 K, with a low velocity range (0–2.5 mm s^{-1}), in order to study the relaxation broadening of the single line of Fe^{2+} and to enable comparisons to be made with the absorber results; and (ii) between 5.5 and 1.3 K, with a larger velocity range (0–3.4 mm s^{-1}), in order to observe in greater detail the appearance of the two additional Fe^{2+} quadrupole doublets.

Figure 6 shows some of the spectra and fitted curves. In the overall temperature range (15–1.3 K) the Fe^{1+} component is present in the emission spectra[3] as a doublet *d* whose characteristics are temperature independent [$S \simeq 1.2$ mm s^{-1} referred to $K_4Fe(CN)_6 \cdot 3H_2O$; $\Delta E \simeq 1.75$ mm s^{-1}; mean linewidth 0.66 mm s^{-1}]. Due to its low relative intensity ($10 \pm 2\%$) and its very large linewidth, this doublet is not clearly apparent on the spectra, but a careful computer analysis shows that it has to be taken into account.

A. Linewidth study

Down to 6 K the Fe^{2+} emission spectrum consists of a single line (*a*) whose width progressively increases between 15 and 8 K with decreasing temperatures, exactly in the same way as for the absorber experiments (see comparative results, Fig. 3). The source and absorber samples were expected to show the same behavior in this temperature range, because in both cases the thermal equilibrium is achieved within the Fe^{2+} electronic levels. That is the condition $W_4 >> 1/\tau$ which is necessary for the level Γ_4 to appear at the Boltzmann equilibrium in the source is fulfilled above 8 K (see Fig. 5), and therefore the relaxation line shape theory given in Sec. IV also holds for the emission spectra in this temperature range.

Between 1.3 and 6 K the width of the central line in the emission spectra is very different from the linewidth observed in the absorber (Fig. 3). This is due to the lack of thermal equilibrium within the Γ_4 and Γ_5 levels in the source sample. The relaxation line shape theory is then no longer valid for the emission spectra. At the lowest temperatures studied, where the relaxation rates between the electronic levels tend to zero, the emission linewidth again becomes closer to the linewidth in the absorber.

B. Study of the two Fe^{2+} quadrupole doublets. Interpretation in terms of metastable contributions of the excited levels Γ_4 and Γ_5

When the temperature is lowered from 5.5 to 1.3 K two additional quadrupole doublets *c* and *b* succes-

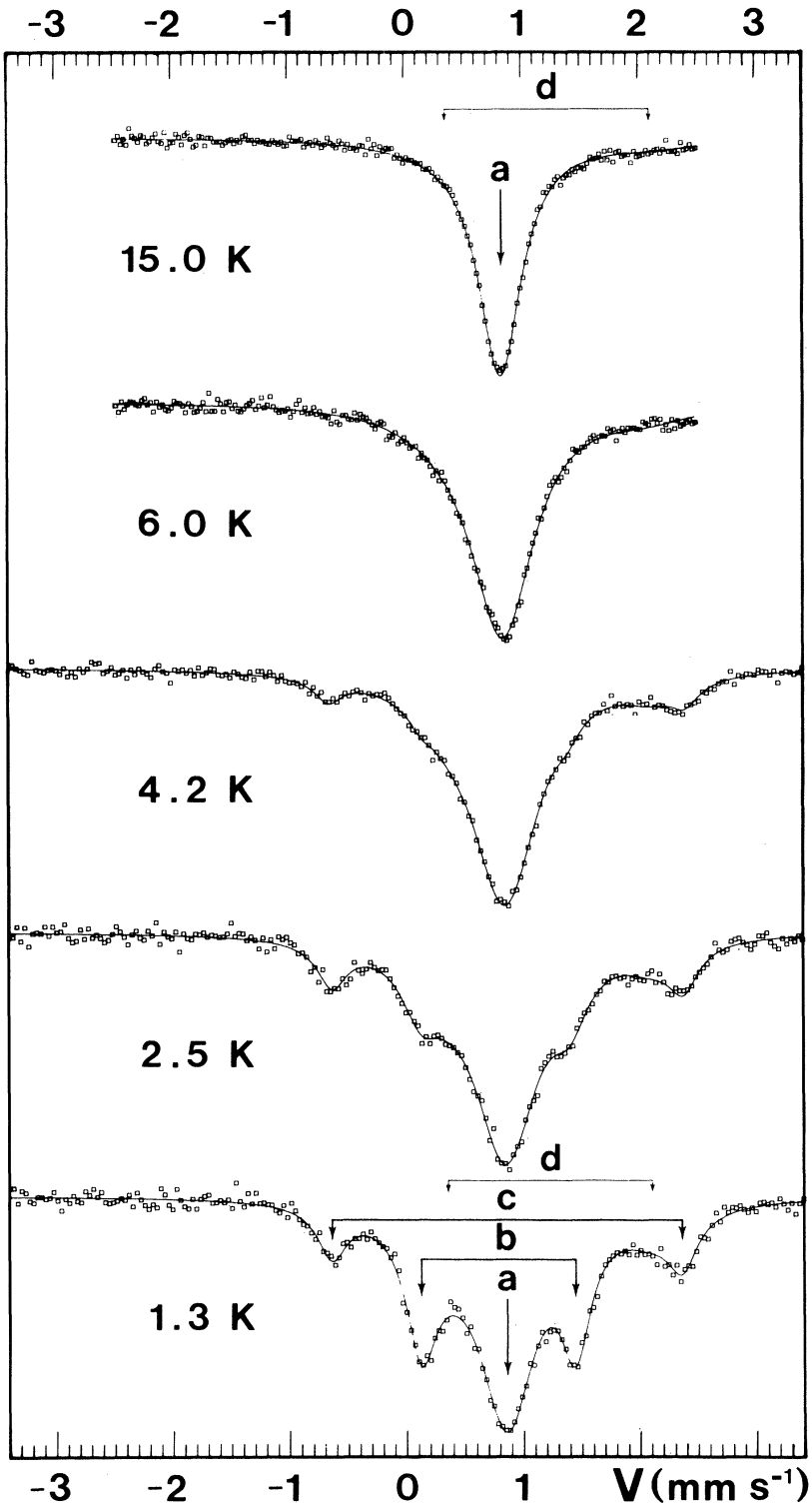

FIG. 6. Mössbauer emission spectra of the source ZnS:^{57}Co and fitted curves. *a*: Fe^{2+} central line; *b*: Fe^{2+} internal quadrupole doublet (Γ_5 contribution); *c*: Fe^{2+} external quadrupole doublet (Γ_4 contribution); and *d*: Fe^{1+} broad doublet [relative intensity $(10 \pm 2)\%$].

sively appear in the emission spectra (Fig. 6). The fitted parameters at 1.3 K are given in Table III. To within the accuracy of the measurements, the isomer shifts of the central line *a* and of the external doublet *c* are the same as the isomer shift of the single Fe^{2+} line in the low-temperature absorption experiments [$S = 0.83 \pm 0.01$ mm s^{-1} referred to $K_4Fe(CN)_6 \cdot 3H_2O$], whereas the isomer shift of the internal doublet *b* is slightly smaller ($S = 0.77 \pm 0.01$ mm s^{-1}). All these isomer-shift values are characteristic of the Fe^{2+} charge state. For both doublets *b* and *c* the isomer shifts, quadrupole splittings, and linewidths do not vary with temperature over the whole range where they are observable. Only their relative intensities are temperature dependent, as shown in Fig. 7.

We assign the doublets *c* and *b* to the metastable slow relaxation contributions of the respective levels Γ_4 and Γ_5.

For the external doublet *c*, this interpretation is supported by the relaxation analysis of the absorber spectra (Sec. IV), which indicated that the Γ_4 level should contribute as a metastable level to the emission spectra below about 4 K because at this temperature $W_4 \sim 1/\tau$. Now Fig. 7 shows that 4 K is precisely the temperature at which the relative intensity P_4 of the doublet *c* is rapidly varying and has a value which is the mean of the value which would correspond to the Boltzmann population in the Γ_4 level [curve $(P_4)_B$] and the low-temperature limiting metastable value.

The internal doublet *b* appears at somewhat lower temperatures (Fig. 7) and its intensity P_5 reaches half the limiting value at about 2.5 K, a temperature at which the Boltzmann population in the Γ_5 level would be negligibly small. Because of the analogy between the behavior of the two doublets *c* and *b*, as well as between the electronic properties of the two excited triplets Γ_4 and Γ_5, the assignment of the doublet *b* to the metastable contribution of the Γ_5 level seems obvious. The comparison between the relaxation measurements in the levels Γ_4 and Γ_5 from the emission spectra (see below) further supports this conclusion.

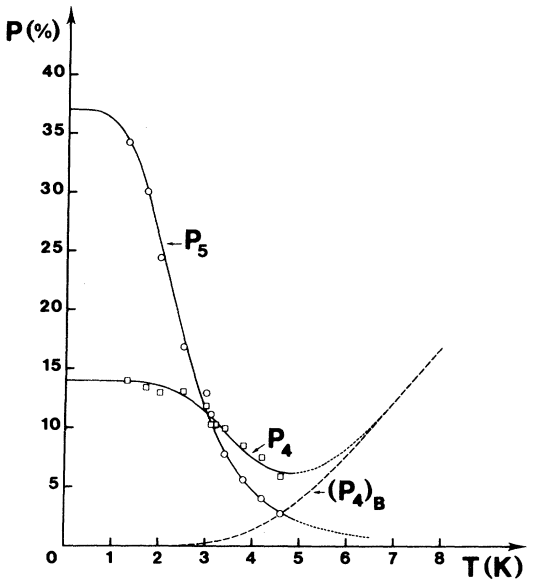

FIG. 7. Relative area of each Fe^{2+} quadrupole doublet in the emission spectra of ZnS:^{57}Co (in percentage of the total Fe^{2+} area). P_4: external quadrupole doublet (Γ_4 contribution); P_5: internal quadrupole doublet (Γ_5 contribution); dashed line curve: relative population $(P_4)_B$ of the level Γ_4 at thermal equilibrium; and full line curves: fitted variations (see Sec. V C).

Finally the coherence of the whole interpretation in terms of metastable contributions of the levels Γ_4 and Γ_5 is examined in the next paper (Part II), where the dynamical Jahn-Teller effect is shown to account for the observed differences between the quadrupole splittings and isomer shift values in the doublets *b* and *c*.

TABLE III. Fitted parameters of the emission spectrum of ZnS:^{57}Co at 1.3 K (Fig. 6). *S*: isomer shift [referred to $K_4Fe(CN)_6, 3H_2O$]; *G*: linewidth; ΔE: quadrupole splitting; and *P*: relative area.

	S (mm s^{-1})	*G* (mm s^{-1})	ΔE (mm s^{-1})	*P* (%)
Fe^{2+} central line (a)	0.84 ± 0.01	0.57 ± 0.02	···	46 ± 2
Fe^{2+} ext. doublet (c)	0.83 ± 0.01	0.32 ± 0.02	3.00 ± 0.03	12.2 ± 1
Fe^{2+} int. doublet (b)	0.77 ± 0.01	0.34 ± 0.02	1.31 ± 0.04	30.1 ± 1
Fe^{1+} doublet (d)	1.20 ± 0.02	0.66 ± 0.10	1.75 ± 0.10	12 ± 2

C. Relaxation measurements

1. Relaxation mechanism

The way in which the external doublet c disappears enables the nature of the responsible relaxation mechanism to be determined.[2]

A relaxation process from Γ_4 towards Γ_1 with an associated transition rate W_4 should induce a noticeable depopulation of the level Γ_4 when $W_4 \sim 1/\tau$, leading to a decrease in the intensity of the doublet c without any appreciable modification of the line shape.

In contrast a relaxation process between the sublevels of Γ_4 with an associated transition rate W_4' should neither modify the population of Γ_4 nor the intensity of the doublet c. But, following Tjon and Blume's line shape theory,[18] this doublet should broaden and it should collapse when $W_4' \gtrsim \Delta E_Q(\Gamma_4)$.

Clearly the experimental results show that the first mechanism with an associated rate W_4 is responsible for the disappearance of the doublet c between 3 and 5 K. This conclusion implies that W_4' cannot be larger than W_4, in agreement with the result obtained at higher temperatures from the absorption measurements which showed that $W_4' << W_4$.

As the doublet b also vanishes without any modification of the line shape, we conclude in the same way that the transitions from Γ_5 to Γ_1 (rate W_5), and not the transitions between the Γ_5 sublevels (rate W_5'), are responsible for the disappearance of this quadrupole doublet between 1.7 and 5 K. This result implies that $W_5' \lesssim W_5$.

2. Measurements of W_4 and W_5

The relaxation line shape theory developed in Sec. IV B was used to measure the relaxation rate W_4 in the absorber when W_4 was roughly comparable to the hyperfine separation $\Delta E_Q(\Gamma_4) = 3.0$ mm s^{-1} (or 219×10^6 s^{-1}). More precisely quantitative information was obtained from this line shape analysis in the range $\frac{1}{10}\Delta E_Q(\Gamma_4) \lesssim W_4 \lesssim 10\Delta E_Q(\Gamma_4)$, i.e., $2.2 \times 10^7 \lesssim W_4 \lesssim 2.2 \times 10^9$ s^{-1} (Fig. 5).

A new method is now available for measuring the transition rate W_4 from the emission spectra, when W_4 is comparable to the natural linewidth $\Gamma = 1/\tau = 7.09 \times 10^6$ s^{-1}: It consists in deducing W_4 from the population of Γ_4, i.e., from the relative intensity of the doublet c in the emission spectra. The same method works too for measuring W_5 from the relative intensity of the doublet b. It will be seen below that the new frequency range thus available is $\Gamma/4 \lesssim W_4$ (or W_5) $\lesssim 4\Gamma$, i.e., $1.8 \times 10^6 \lesssim W_4$ (or W_5) $\lesssim 2.8 \times 10^7$ s^{-1}.

The relation between the transition rate W_4 (or W_5) and the population of the Γ_4 (or Γ_5) level, as observed in the emission spectra, is easily calculated.

Let $t = 0$ be the time at which the radioactive parent ^{57}Co decays. The electronic rearrangement leading to the ground term $^5D_4$ of the Fe^{2+} $3d^6$ configuration is very short compared to the nuclear lifetime $\tau = 1.411 \times 10^{-7}$ s,[22] and it can be neglected in our problem. We also assume that all the electronic levels of Fe^{2+} except the metastable levels Γ_4 and Γ_5 decay towards the ground state level Γ_1 in a time much shorter than τ at the temperature of the experiments ($T < 5$ K). The initial electronic populations of Fe^{2+} are thus supposed to be, respectively, $P_1(0)$, $P_4(0)$, and $P_5(0)$ in the levels Γ_1, Γ_4, Γ_5 immediately after the decay of ^{57}Co. It can be further supposed that there is no appreciable population transfer from the Γ_5 level to the Γ_4 level, as the Γ_4 population does not increase between 1.3 and 2.5 K when the Γ_5 population abruptly decreases (Fig. 7).

The evolution of the population $P_4(t)$ of the triplet Γ_4 as a function of the time t during the nuclear lifetime is then given by

$$\frac{dP_4(t)}{dt} = -P_4(t)\,W_4 + 3P_1(t)\,W_4 \exp(-\delta/k_B T) \quad . \tag{5.1}$$

In the last term, $P_1(t) = 1 - P_4(t) - P_5(t)$ can be approximated by $1 - P_4(t)$ because $P_5(t)$ reduces to zero in a time $t << \tau$ above 4 K (Fig. 7), whereas the multiplicative factor $\exp(-\delta/k_B T)$ vanishes below 4 K.

The solution of the evolution equation (5.1) is given by

$$P_4(t) - (P_4)_B = [P_4(0) - (P_4)_B] \exp[-W_4(1 + 3e^{-\delta/k_B T})t] \quad ,$$

where $(P_4)_B$ represents the population of the level Γ_4 at the Boltzmann equilibrium

$$(P_4)_B = \frac{3e^{-\delta/k_B T}}{1 + 3e^{-\delta/k_B T}} \quad . \tag{5.2}$$

To obtain the actual population P_4 which corresponds to the relative intensity of the external doublet c in the Fe^{2+} Mössbauer emission spectra, we need to find the average of $P_4(t)$ over a time t for the exponential decay of the 14.4-keV excited level of ^{57}Fe:

$$P_4 - (P_4)_B = \frac{1}{\tau}\int_0^\infty [P_4(t) - (P_4)_B] e^{-t/\tau} dt$$

which gives

$$W_4 = \frac{1}{\tau}\frac{1}{1 + 3e^{-\delta/k_B T}}\frac{P_4(0) - P_4}{P_4 - (P_4)_B} \quad . \tag{5.3}$$

A similar law relates the depopulation rate W_5 of the level Γ_5 to the population P_5 which is given by the relative intensity of the internal doublet b. As the Boltzmann factor relative to the level Γ_5 is completely

negligible below 5 K, the result can be simply written

$$W_5 = \frac{1}{\tau}\frac{P_5(0)-P_5}{P_5} \quad . \tag{5.4}$$

[In relations (5.3) and (5.4) τ is supposed to be the mean lifetime $\tau = t_{1/2}/\ln 2 = 1.411 \times 10^{-7}$ s of the 14.4-keV state of ^{57}Fe. In fact the decay of ^{57}Co first leads to the 136-keV level of ^{57}Fe, which then decays into the 14.4-keV level. As the mean life $\tau' = 0.126 \times 10^{-7}$ s of the 136-keV state is much shorter than τ,[22] it could be neglected as a first approximation. However we used a better approximation which consists in introducing an effective mean time τ_e instead of τ in relations (5.3) and (5.4), with $\tau_e = \tau + \tau' = 1.537 \times 10^{-7}$ s.]

The initial populations $P_4(0)$ and $P_5(0)$ result from a complex electronic cascade which follows the decay of ^{57}Co, and there is at present no way for these populations to be calculated. However in the zero-temperature limit, the relations (5.3) and (5.4) give

$$P_4(0) = (P_4)_{T\to 0}[1 + \tau W_4(T\to 0)] \quad , \tag{5.5}$$

$$P_5(0) = (P_5)_{T\to 0}[1 + \tau W_5(T\to 0)] \quad . \tag{5.6}$$

Extrapolation of W_4 obtained from the absorber measurements towards low temperatures shows that W_4 probably becomes smaller than $\frac{1}{10}(1/\tau)$ below around 2.5 K, and smaller than $\frac{1}{100}(1/\tau)$ below around 1.6 K. At the zero-temperature limit the condition $\tau W_4(T\to 0) \ll 1$ is thus certainly fulfilled, and Eq. (5.5) reduces to $P_4(0) = (P_4)_{T\to 0}$: so the value of $P_4(0)$ corresponds to the limiting population P_4 of Γ_4 which is observed at low temperature, i.e., $P_4(0) \simeq 0.14$ (Fig. 7).

By admitting that $\tau W_5(T\to 0)$ is also negligibly small compared to unity, we obtain in the same way $P_5(0) = (P_5)_{T\to 0}$. As P_5 is not completely saturated at the lowest measurement temperature (1.3 K), the extrapolated value $(P_5)_{T\to 0} \simeq 0.37$ is known to within an uncertainty of ± 0.02.

Using the relations (5.3) and (5.4) with these values $P_4(0) = \frac{14}{100}$ and $P_5(0) = \frac{37}{100}$, and the population measurements P_4 and P_5 given in Fig. 7, we calculated the corresponding relaxation rates W_4 and W_5 at various temperatures. The results are shown on Fig. 5 and in Table II with the notation "source experiments."

We observe a very good compatibility between the source measurements and the absorber measurements of W_4 in that on the log-log plot of Fig. 5 all the W_4 measurements follow a straight line over the whole temperature range (3–13 K). This line corresponds to the fitted law

$$W_4(\mathrm{s}^{-1}) = 6.77 \times 10^3 T^{5.0} \quad . \tag{5.7}$$

The source measurements of W_5 between 1.7 and 4.6 K are in turn compatible with a straight line curve corresponding to the fitted law

$$W_5(\mathrm{s}^{-1}) = 0.178 \times 10^6 T^{4.0} \quad . \tag{5.8}$$

In the opposite way, if we use Eqs. (5.7) and (5.8), we can calculate the populations P_4 and P_5 by means of Eqs. (5.3) and (5.4). These calculated population variations are shown by the solid lines in Fig. 7, and they are again in good agreement with the directly measured populations.

D. Origin of the relaxation processes W_4 and W_5

When interpreting the origin of the transition rates W_4 and W_5, it must be kept in mind that they present a very unusual characteristic. Namely, they are observed at temperatures which are smaller (or much smaller) than the energy difference between the relevant electronic levels Γ_4 and Γ_1 (or Γ_5 and Γ_1).

The Raman processes are known to give a T^x thermal dependence of the relaxation rate, with $x = 7$ in the case of non-Kramers levels.[23] As we observe here a T^x-type law, but with $x < 7$, we reexamined the calculation of the transition probability $W^R_{e\to g}$ due to Raman processes from one excited level to the ground-state level, when the energy separation $E_e - E_g = \hbar\omega_0$ is larger than $k_B T$. The usual T^7 dependence results from the integration in the Debye approximation of[23]

$$W^R_{e\to g} \propto \int_0^{\omega_D} d\omega_1 n(\omega_1)[n(\omega_2)+1]\omega_1^3\omega_2^3 \quad ,$$

where the two phonons $\hbar\omega_1$ and $\hbar\omega_2$ are supposed to have the same energy ($\hbar\omega_1 = \hbar\omega_2$). But, for $kT \lesssim \hbar\omega_0$, the exact energy conservation relation $\hbar\omega_2 = \hbar\omega_1 + \hbar\omega_0$ is required. Instead of

$$W^R_{e\to g} \propto I^6\left(\frac{k_B T}{\hbar}\right)^7 \quad ,$$

where

$$I^n = \int_0^{\theta_D/T} \frac{x^n e^x dx}{(e^x-1)^2} \simeq n! \quad \text{if} \quad T < \frac{\theta_D}{10}$$

the exact result is now the linear combination of four power terms:

$$W_{e\to g}^{R} \propto (\omega_0)^7 \left[I^6 \left(\frac{k_B T}{\hbar \omega_0} \right)^7 + 3I^5 \left(\frac{k_B T}{\hbar \omega_0} \right)^6 + 3I^4 \left(\frac{k_B T}{\hbar \omega_0} \right)^5 + I^3 \left(\frac{k_B T}{\hbar \omega_0} \right)^4 \right]$$

or

$$W_{e\to g}^{R} \propto (\omega_0)^7 \left[120 \left(\frac{k_B T}{\hbar \omega_0} \right)^7 + 60 \left(\frac{k_B T}{\hbar \omega_0} \right)^6 + 12 \left(\frac{k_B T}{\hbar \omega_0} \right)^5 + \left(\frac{k_B T}{\hbar \omega_0} \right)^4 \right] . \tag{5.9}$$

When applied to the W_4 relaxation rate between 3 and 13 K, this law can be approximated by the averaged law $W_{e\to g}^{R} \propto T^{5.78}$ in this temperature range, which is to be compared to the experimental law $W_4 \propto T^{5.0}$.

In a similar way, when applied to the relaxation rate W_5 between 1.7 and 4.6 K, the law (5.9) can be approximated by $W_{e\to g}^{R} \propto T^{4.48}$, which is to be compared to the experimental law $W_5 \propto T^{4.0}$.

In both cases the calculated Raman thermal variation is not very different from the experimental variation, although the calculated exponent x is somewhat larger than the experimental value.

This small difference probably results from the use of the Debye approximation in the calculation. The interpretation of the relaxation rates in terms of low-temperature Raman processes is further supported by the order or magnitude of the ratio W_5/W_4. With the reasonable assumption that the levels Γ_4 and Γ_5 have comparable transition matrix elements towards the ground-state level Γ_1, i.e., assuming identical proportionality coefficients in relation (5.9) for both levels Γ_4 and Γ_5, the calculated ratio at $T = 3$ K is $W_5/W_4 \simeq 11$, in good agreement with the experimental value $(W_5/W_4)_{\text{expt}} = 8.8$ at the same temperature.

The other possible relaxation mechanisms that can be invoked cannot account for the experimental results.

Direct processes correspond to a transition probability[23]

$$W_{e\to g}^{D} \propto \frac{\omega_0^3}{1 - \exp(-\hbar\omega_0/k_B T)} \tag{5.10}$$

giving a temperature-independent contribution $W^D(0)$ for $k_B T \ll \hbar\omega_0$. If an appreciable direct contribution were present in our measurements, it would mean that the $\tau W^D(0)$ terms would be not much smaller than unity, and this would require a revision of the procedure used when calculating $P_4(0)$ or $P_5(0)$ from the relations (5.5) and (5.6). However the introduction of an appreciable $\tau W_4(T \to 0) = \tau W_4^D(0)$ term in Eq. (5.5) leads to a discrepancy between the source and the absorber measurements of W_4, and it must be discarded. For W_5 where no absorber measurements exist, we introduced tentative finite values of $\tau W_5(T \to 0) = \tau W_5^D(0)$ in Eq. (5.6), which gave modified values of $P_5(0)$. The relation (5.4) gave in turn new thermal variations of W_5, which have been fitted by adding the direct contribution value $W_5^D(0)$ to an adjustable Raman contribution according to Eq. (5.9). As the fit is not improved by using finite values of $W_5^D(0)$, we think that the direct relaxation processes probably do not play any role in the measurements of W_5.

In addition, Orbach relaxation processes cannot account for the observed thermal variations of W_4 and W_5.

As a conclusion we think that the dominant contributions to the observed relaxation rates W_4 and W_5 are due to Raman processes, which to a first approximation follow the low-temperature behavior given by Eq. (5.9).

VI. CONCLUSION

It should be emphasized first that the careful study of the relaxation phenomena of the Fe^{2+} ion in ZnS supports the interpretation of the complex emission Mössbauer spectra near 0 K in terms of contributions from metastable, excited, spin-orbit levels whose populations remain out of thermal equilibrium after the decay of the radioactive parent.

For the contribution of the Γ_4 level this conclusion follows from the analysis of the relaxation rates obtained from the line shape in the absorption spectra of Fe^{2+} in ZnS, which shows that below 4 K the transition from the state Γ_4 to the ground state Γ_1 requires a time longer than the nuclear lifetime τ. Now it is precisely near 4 K that we observe a rapid thermal variation of the line intensity of the external doublet in the source spectra. As in addition this doublet presents the characteristics predicted by Ham for the slow relaxation contribution of the level Γ_4, its assignment to this level is obvious.

Despite the fact that for the Γ_5 level direct evidence based on the analysis of the absorption spectra is not available, the assignment of the internal doublet in the emission spectra to the level Γ_5 is well established: the comparison between the thermal behaviors of the relaxation rates W_4 and W_5, as well as the observed value of the ratio W_5/W_4, support the conclusion of the Jahn-Teller study (Part II, next paper) which attributes the two quadrupole doublets to the two closely related spin-orbit levels Γ_4 and Γ_5.

The existence of such abnormal electronic populations in emission Mössbauer spectra, which seem to be unambiguously observed here for the first time, presents several interesting and unconventional aspects.

First this effect has enabled the slow relaxation spectra of two excited levels to be observed and studied independently near 0 K, whereas at the temperatures required to obtain sizable thermal populations of these same levels the relaxation rates fall in the intermediate to fast range. Now slow relaxation hyperfine structures generally provide much more information than that provided by a fast relaxation averaged spectrum, which reduces into a single line in the ZnS:Fe^{2+} system. As will be shown in Part II, the observation of the slow relaxation hyperfine contributions of the Γ_4 and Γ_5 levels in the emission spectra enables an evaluation to be made of the Jahn-Teller coupling between the vibrational modes and the various spin-orbit levels of the ^5E state of the Fe^{2+} ion in ZnS.

Another interesting feature is related to the possibility of deducing electronic relaxation rates from line intensity measurements in emission Mössbauer spectroscopy. This possibility can be considered as opening a "new window" for measuring relaxation rates: the frequency range thus accessible is centered around the value $\Gamma = 1/\tau$ (the natural linewidth) instead of the value ω_{hf} (the hyperfine separation) as for the usual relaxation line shape measurements. This possibility has been experimentally demonstrated by measuring the transition rates W_4 and W_5 from the emission spectra of Fe^{2+} in ZnS.

It should be mentioned that a similar treatment for obtaining relaxation rates from line intensity variations in emission spectra was used a few years ago for studying ^{170}Yb impurities in a gold matrix.[24] The main difference between the two types of experiments rests in the nature of the levels which are observed out of the thermal equilibrium: namely, the electronic levels in the case of Fe^{2+} in ZnS and the hyperfine levels in the case of ^{170}Yb in gold. Another difference lies in the fact that the initial populations of the relevant levels after the decay of the radioactive parent were known from theoretical reasons in the case of *Au*Yb, but were not known *a priori* in the case of ZnS:Fe^{2+}.

Whereas the theory of emission Mössbauer spectra in the presence of relaxation has been worked out by Hartmann-Boutron[25] and Afanasev and Gorobchenko,[26] Hirst *et al.*[27] have mentioned the interesting possibility of studying relaxation phenomena from *electronic population measurements* in a Mössbauer source, but their line shape calculations were not correct[28] and they used a nonconvincing experimental example, namely, the central contribution observed in the *Au*^{166}Er spectra, which in fact probably comes from clustering effects rather than from an excited crystal-field level.

The "new window" for measuring relaxation rates which is opened by line intensity measurements in emission Mössbauer spectroscopy, presents some analogy with the widely used "pulse-saturation method" in EPR impurity studies: a perturbation is applied to the resonant atom, i.e., radio-frequency pumping between electronic Zeeman levels in EPR analogous to the radioactive decay of the Mössbauer nucleus in emission Mössbauer spectroscopy, leaving the electronic or hyperfine populations out of thermal equilibrium. One then measures the recovery of the system towards equilibrium. The main difference between the two techniques lies in the nature of the delay time t between the application of the perturbation and the measurement. In EPR t is chosen by the experimentalist, and extracting the relaxation rate requires measurements at various values of t; in emission Mössbauer spectroscopy the mean value of t is equal to the nuclear lifetime τ, and a unique measurement yields the relaxation rate, once the initial populations are known. In the same way the usual Mössbauer effect method for measuring relaxation rates, i.e., by means of studying the deformation of the line shape, is analogous to the EPR linewidth measurement: both are "steady state methods" without perturbation of the resonant atom. It is worth noticing that for both the EPR and the Mössbauer techniques the perturbation method ("new window") allows measurements to be made in a lower-temperature range than for the steady state method.

Some specific features of the present relaxation study on the system ZnS:Fe^{2+} are to be emphasized. First, contrary to the EPR, the Mössbauer technique does not require the use of an applied magnetic field, and the relaxation was observed in the absence of any magnetic perturbation on the levels. Secondly, the source experiments were carried out at temperatures k_BT much lower than the energy $\hbar\omega_0$ of the observed excited levels (the Γ_4 or Γ_5 levels). This is a nonconventional temperature range for relaxation measurements. We thus reexamined the thermal behavior of the Raman relaxation rates for the case $k_BT < \hbar\omega_0$ and we showed that the transition rate from the excited level towards the ground-state level then follows the variation $W_{e\to g} \propto 120(k_BT/\hbar\omega_0)^7 + 60(k_BT/\hbar\omega_0)^6 + 12(k_BT/\hbar\omega_0)^5 + (k_BT/\hbar\omega_0)^4$ instead of the classical T^7 variation.

As a final remark, some other experiments could be suggested following the present study. It would be interesting first to examine the source ZnS:^{57}Co by means of coincidence Mössbauer spectroscopy in the vicinity of the liquid helium temperature, as the relative intensities of the lines due to the metastable levels should change as a function of the observation time, i.e., of the delay time in the coincidence. It could be worthwhile too to extend the present meas-

urements to other ^{57}Co sources producing Fe^{2+} ions in tetrahedral coordination, such as ^{57}Co sources in cubic ZnSe, ZnTe, and CdTe matrices or in spinel-type compounds.

We are presently studying the source CaF_2:^{57}Co, as previous relaxation measurements in a CaF_2:^{57}Fe absorber have already shown that the level Γ_4 of Fe^{2+} should appear as a metastable level in this source below about 15 K.[21]

Finally systematic comparative studies of Mössbauer absorption and emission spectra of Fe^{2+} compounds or of rare-earth compounds containing low lying electronic levels could reveal the metastable character of some of these levels and enable their slow relaxation contributions to be observed in emission spectroscopy near 0 K.

ACKNOWLEDGMENTS

We thank C. Carcaillet, S. Legrand, and R. Saint-James for preparing the absorber samples; Dr. J. Danon and Dr. M. Cottin for help with the source sample preparation and for discussions concerning the after-decay effects; N. Genand-Riondet and J. F. Lericque for help with the Mössbauer experiments; and Dr. J. A. Hodges for useful remarks concerning this work and for comments on the manuscript. One of us (A. G.) wishes to express his gratitude to the Ministère des Affaires Etrangères de Belgique, for financially supporting his collaboration with the Centre d'Etudes Nucléaires de Saclay in France.

---

*Institut de Physique, Université de Liège-Sart Tilman, B4000 Liège, Belgique.

[1]V. I. Goldanskii and R. H. Herber, *Chemical Applications of Mössbauer Spectroscopy* (Academic, New York, 1968), p. 614.

[2]C. Garcin, P. Imbert, and G. Jéhanno, Solid State Commun. 21, 545 (1977).

[3]C. Garcin, A. Gérard, P. Imbert, G. Jéhanno, and J. Danon, J. Phys. Chem. Solids 41, 969 (1980).

[4]F. S. Ham, J. Phys. (Paris) Suppl. 35, C6-121 (1974).

[5]P. Imbert, C. Garcin, G. Jéhanno, and A. Gérard, in *International Conference on Mössbauer Spectroscopy, Bucharest, 1977,* edited by D. Barb and D. Tarina (Central Institute of Physics, Bucharest, Romania, 1977), Vol. II, p. 123.

[6]G. A. Slack, F. S. Ham, and R. M. Chrenko, Phys. Rev. 152, 376 (1966).

[7]J. T. Vallin, Phys. Rev. B 2, 2390 (1970).

[8]M. H. L. Pryce, Phys. Rev. 80, 1107 (1950).

[9]J. T. Vallin, G. A. Slack, and C. C. Bradley, Phys. Rev. B 2, 4406 (1970).

[10]P. Bonville, C. Garcin, P. Imbert, and G. Jéhanno, J. Phys. (Paris) Colloq. 41, C1-237 (1980).

[11]A. Gérard, P. Imbert, H. Prange, F. Varret, and M. Wintenberger, J. Phys. Chem. Solids 32, 2091 (1971).

[12]J. R. Régnard and J. Chappert, J. Phys. (Paris) Colloq. 37, C6-611 (1976).

[13]J. R. Régnard and U. Dürr, J. Phys. (Paris) 40, 997 (1979).

[14]H. R. Leider and D. N. Pipkorn, Bull. Am. Phys. Soc. 11, 49 (1966); Phys. Rev. 165, 494 (1968).

[15]R. B. Frankel and N. A. Blum, Bull. Am. Phys. Soc. 12, 24 (1967).

[16]J. Chappert, R. B. Frankel, and N. A. Blum, Bull. Am. Phys. Soc. 12, 352 (1967); Phys. Lett. 25A, 149 (1967).

[17]F. S. Ham, Phys. Rev. 160, 328 (1967).

[18]J. A. Tjon and M. Blume, Phys. Rev. 165, 456 (1968).

[19]M. Blume, Phys. Rev. 174, 351 (1968).

[20]M. J. Clauser, Phys. Rev. B 3, 3748 (1971).

[21]P. Bonville, J. Chappert, C. Garcin, P. Imbert, and J. R. Régnard, J. Phys. (Paris) Colloq. 41, C1-235 (1980).

[22]*Mössbauer Effect Data Index,* edited by J. G. Stevens and V. E. Stevens (Plenum, New York, 1976).

[23]K. W. H. Stevens, Rep. Prog. Phys. 30, 189 (1967).

[24]F. Gonzalez-Jimenez, F. Hartmann-Boutron, and P. Imbert, Phys. Rev. B 10, 2122 (1974).

[25]F. Hartmann-Boutron, Phys. Rev. B 10, 2113 (1974).

[26]A. M. Afanasev and V. D. Gorobchenko, Phys. Status Solidi B 73, 73 (1976).

[27]L. L. Hirst, J. Stöhr, G. K. Shenoy, and G. M. Kalvius, Phys. Rev. Lett. 33, 198 (1974).

[28]L. L. Hirst, J. Phys. (Paris) Colloq. 35, C6-21 (1974).